A COMPARISON OF THE RANS AND LES TURBULENCE MODELS IN THE SIMULATION OF EMISSIONS FROM FLARES TO THE ENVIRONMENT.

Aboje A. A.

Department of Chemical Engineering, Federal University of Technology, PMB 65 Minna, Nigeria.
alen248@futminna. edu.ng

ABSTRACT

Purpose: This study is an attempt to simulate wake-stabilized flares in the petroleum and gas industry using mathematical equations governing the flow, turbulence and combustion in flames as encoded in the ANSYS-HYSYS simulation software package. The work compares the RANS and LES turbulence models in conjunction with the partially premixed combustion model. The model uses the mixture fraction approach in order to predict the flame appearance and the thermochemical properties of the wake stabilized cross flow flame.

Design/ Methodology/ Approach: The research strategy involves using the RANS (Reynolds Averaged Navier Stokes) and the LES (Large Eddy Simulation) mathematical Models to simulate and to study the physical structure and the thermochemical properties of natural gas flares in the presence of crosswind. The wind-tunnel geometry was built and meshed using the ICEM software, the calculations were carried out in the ANSYS-Fluent CFD software and the computational data generated was processed and analyzed using the Tecplot CFD post-processing software package. The results of the simulation were then validated against the experimental work of Huang and Wang.

Findings: The findings demonstrated that the LES turbulence model outperformed the RSM turbulence model in terms of predicting temperature trends and pollutant species. However, the peak temperatures at the analyzed measurement locations were predicted by both models accurately. The LES model also improved CO_2 concentration predictions. In general, the LES turbulence model predicts more accurately than the RANS model, but the RANS model still provides a respectably accurate forecast of the thermo-chemical characteristics of the flame, making it a viable substitute for the more expensive LES.

Practical Implications: The practical implications of the work is that simulation can be used in place of experiments to save money on some of the more expensive experimental projects since the results from the simulation agrees fairly well with the experimental data.

Social Implications: Gas flaring has caused a lot of environmental damage in the Niger Delta area of Nigeria and other parts of the third world where the gas flaring menace has been a concern. The availability of simulation codes to investigate the pollution from the flares will go a long way in mitigating the effects of this pernicious industrial practice.

Originality and Value: Previous works that have been done with gas flares have focused mainly on methane but this work focuses on propane which is also an important constituent of natural gas.

Keywords: *flares, diffusion flames, pollutant species, turbulence models, combustion models*

C. Aigbavboa et al. (Eds.): Sustainable Education and Development, pp. 818-832, 2024.
https://doi.org/10.1007/978-3-030-68836-3 1

1. INTRODUCTION

Gas flaring is the act of disposing surplus flammable gases and vapors by combusting them in the open atmosphere. These include flares from onshore and offshore petroleum production activities, petroleum refineries, chemical and petrochemical plants, natural gas processing plants, landfills and anything accommodating pressurized hydrocarbons. This process is affiliated with the undesirable formation of pollutants, such as CO, NOx, smoke, unburned hydrocarbons and CO_2 (John, 2023). Flaring is not as damaging to the environment as gas venting because based on reports by the IPCC

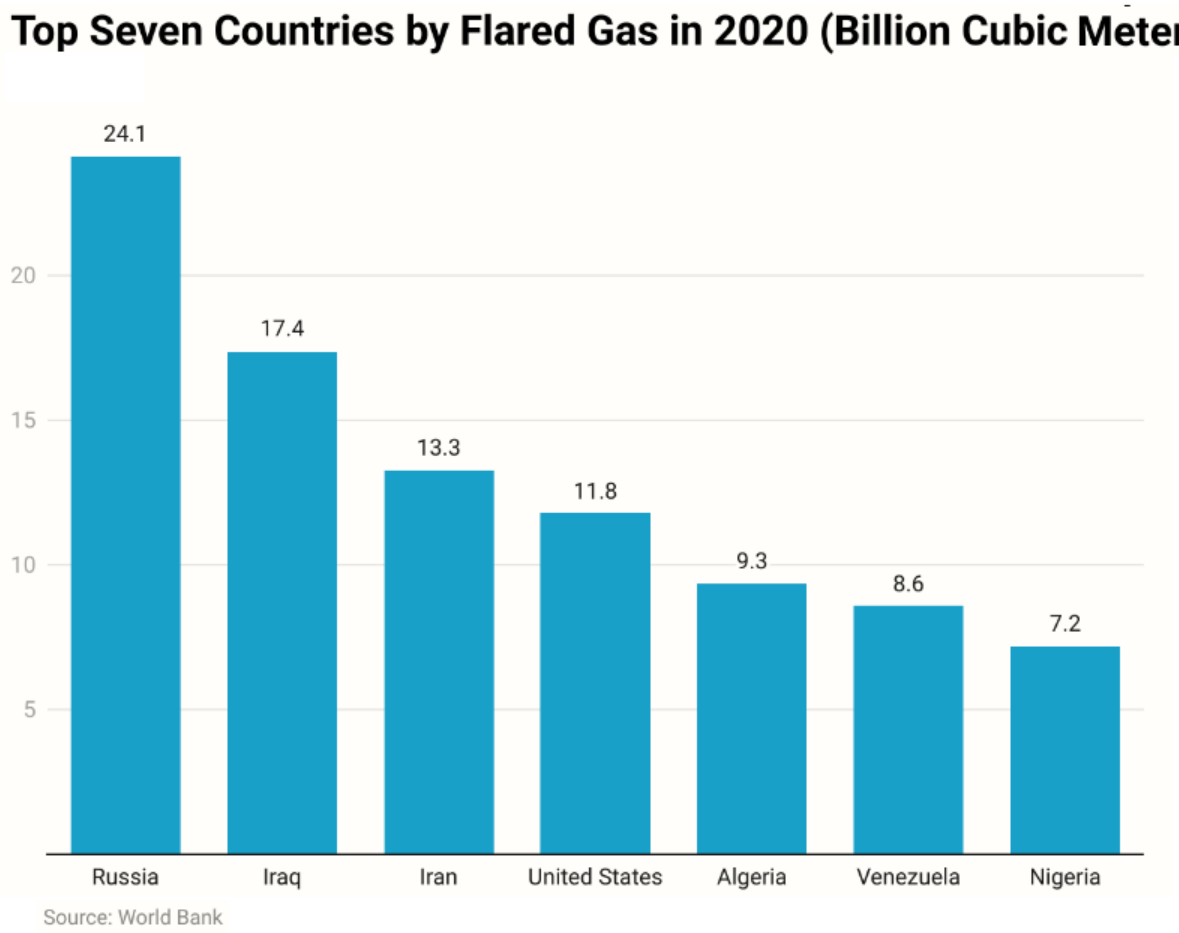

Figure 1. Bar chart of Top 7 gas flaring nations as of 2020

for instance, it has been shown that over a 100-year period, methane, a key component of natural gas, is about 25 times more efficient than carbon dioxide at trapping heat in the atmosphere. Methane has a 25-fold more potential to cause global warming than carbon dioxide, to put it another way. (Sullivan, 2023). Therefore burning methane and other hydrocarbons that constitute natural gas is a better option than venting. Experimental works on the combustion of methane, which is a major component of onshore and offshore oil and gas rigs, has been studied by several researchers in the past (Bandaru & Turns, 2000; Botros & Brzustowski, 1979; Escudier, 1971, Eric et al., 2022; Ilya et al., 2022; Paul et al.,

C. Aigbavboa et al. (Eds.): Sustainable Education and Development, pp. 818-832, 2024.
https://doi.org/10.1007/978-3-030-68836-3 1

2021). However, the combustion of propane and other hydrocarbons which are equally important has received less attention. This work therefore focuses on the combustion of propane, which constitutes a significant proportion of refinery flare gases as well as some offshore and onshore flaring sites. Nevertheless some notable experimental work has been done on the combustion of propane. This includes the works done by Gollahalli & Nanjundappa (1995)where they investigated propane flames in a cross flow of air for different jet-to-cross flow momentum ratios related to gas flares operating in the wake-stabilized regime, which is the regime where the momentum of the crossflow dominates both the buoyancy and the fuel jet momentum. In-depth experimental work on propane flames in a cross-flow of air was also carried out by Huang & Yang (1996), who looked at the flames' structure in various regimes as well as their species concentration and temperature field. Numerical simulation of flames have received increased attention in recent years due to the increase in computer processing power, however majority of the work done have been on methane flames (Castineira & Edgar, 2008; Lawal et al., 2010, 2013).The current work simulates propane combustion using the existing combustion, flow, turbulence, and radiation models in the ANSYS package and the results have been validated using data from the work of Huang and Yang (1996). The top 10 gas-flaring nations accounted for 75% of all gas flared, according to the 2022 Global Gas Flaring Tracker Report from the Global Gas Flaring Reduction Partnership (GGFR), a prominent international and independent indicator of gas flaring (John, 2023). Seven of the top 10 countries for flare-ups have maintained their ranking over the past ten years: Russia, Iraq, Iran, the United States, Algeria, Venezuela, and Nigeria. Figure 1 gives the most recent statistics on the volume of gas flared by each of these countries, with the total annual flare volume peaking at around 150 billion cm^3. The last three in the top 10; Mexico, Libya, and China, have demonstrated a noticeable increase in flaring in recent years.

2. METHODOLOGY

2.1 Numerical Methods

To simulate the flow, the turbulence, and the combustion, mathematical models from the commercial CFD software program ANSYS-Fluent R2 (2020) were utilized. The codes use the finite volume solution approach to solve the balance equations for mass, momentum, energy, and the pertinent scalar parameters defining turbulence and combustion in their Favre-averaged form. The flow field was modeled based on the Reynolds-Averaged Navier-Stokes (RANS) equation. The Reynolds Stress Model Model(Launder et al., 1975)and the Large Eddy Simulation Model (Ferziger, 1976)have been used to resolve the Reynolds stresses resulting from the RANS equation, and the findings from the twoturbulence models have been compared. Combustion was modeled based on the partially premixed

C. Aigbavboa et al. (Eds.): Sustainable Education and Development, pp. 818-832, 2024.
https://doi.org/10.1007/978-3-030-68836-3 1

model (Pierce & Moin, 2004) and radiation (which manifests as a drain in the energy equation) was modeled based on the Discrete Ordinate Model (Fiveland, 1984). Soot formation was modelled based on the Moss-Brookes-Hall model (Hall et al., 1999) while the kinetics of the propane reaction was modeled based on the CRECK reaction mechanism of Ranzi et al. (2012). The research strategy involves using the RANS and the LES Models to simulate and study the physical structure and the thermochemical properties of natural gas flares in the presence of crosswind. The wind-tunnel geometry was built and meshed using the ICEM software. The calculations were carried out in the ANSYS-Fluent CFD software and the computational data generated was processed and analyzed using the Tecplot CFD post-processing software package. Sampling was done by investigating different locations in the flame in order to determine the structure and the thermochemical predictions of the flame. The results of the simulation were then validated against the experimental work of Huang and Wang.

Conservation equations

Below in Cartesian tensor notation is a brief explanation of the governing equations for the study of turbulent reacting flows.

Mass conservation:

$$\frac{\partial \bar{\rho}}{\partial t} + \frac{\partial}{\partial x_k}(\bar{\rho}\tilde{u}_k) = 0 \quad (1)$$

Momentum conservation:

$$\frac{\partial(\bar{\rho}\tilde{u}_i)}{\partial t} + \frac{\partial}{\partial x_k}(\bar{\rho}\tilde{u}_k\tilde{u}_i) = \frac{\partial \bar{P}}{\partial x_i} + \frac{\partial \tau_{ik}}{\partial x_k} + \tilde{F}_k - \frac{\partial}{\partial x_k}\left(\rho\widetilde{u_k''u_i''}\right) \quad (2)$$

wherethe symbol ~denotes a Favre mean, or density weighted mean quantity, the symbol ″ represents a fluctuating quantity while $\bar{P}$ and $\bar{\rho}$are the unweighted pressure and density. The two terms on the left of equation (2) denotes the accumulation and the convective terms respectively. The first three terms on the right denotes the pressure, the viscous and source terms, respectively, while the last term represents the turbulence or the Reynolds stress.

Energy conservation:

$$\frac{\partial}{\partial t}(\rho h) + \frac{\partial}{\partial x_j}\left(\rho h u_j\right) = \frac{\partial}{\partial x_j}\left(\frac{\mu}{Pr}\frac{\partial h}{\partial x_j}\right) + q_{rad} \quad (3)$$

where $Pr$and $h$are the Prandtl number and the specific enthalpy of the mixture, whileq_{rad} is the source term due to the radiation heat loss.

C. Aigbavboa et al. (Eds.): Sustainable Education and Development, pp. 818-832, 2024.
https://doi.org/10.1007/978-3-030-68836-3 1

Turbulencemodels

The turbulent viscosity and the gradient transport theory that are required by Eddy viscosity models are not required here because the Reynolds stress transport model directly solves the transport equation for the turbulent or Reynolds stresses. Symbolically, the Reynolds stress transport model can be expressed as

$$\frac{\partial}{\partial t}\left(\rho\overline{u_i'u_j'}\right) + \frac{\partial}{\partial x_k}\left(\rho u_k\overline{u_i'u_j'}\right) = D_{ij} + P_{ij} + G_{ij} + \phi_{ij} - \varepsilon_{ij} - F_{ij} \quad (4)$$

where the first and the second terms on the left are the transience and convection terms, respectively. The six terms on the right are the diffusion, shear production, buoyancy production, redistribution, dissipation and system rotation production terms, respectively. The term for the pressure strain correlation,$\phi_{ij}$is responsible for of pressure fluctuation effects, which makes the turbulence more isotropic by redistributing it among the other components. The Navier-Stokes equation is directly solved in real time using the LES approach for large scale eddies, although subgrid scale models are used to describe the lower size eddies. The are many models that are available for approximating the subgrid scale stresses that result from the filtering operation, however the Smagorinsky model (Smagorinsky, 1963)is widely adopted and it is used here. The filtering equation is defined as:

$$\begin{aligned} \bar{\Delta}G(x - x^*) &= 1 \qquad |x - x^*| < \bar{\Delta} \\ &= 0 \qquad |x - x^*| > \bar{\Delta} \end{aligned} \quad (5)$$

and the large eddies that are resolved have filter width >$\bar{\Delta}$ while the smaller eddies that are discarded and are later modeled have filter <$\bar{\Delta}$.

Combustion model and Reaction mechanism

The combustion of the flame was modeled using the partially premixed combustion model. Premixed and non-premixed flame characteristics can both be seen in partially premixed flames. They happen when a diffusion flame becomes lifted, causing some premixing to take place before combustion. A progress variable, C, which tracks the overall extent of the reaction, and a mixture percent variable, Z, which tracks the mixing of the fuel and oxidizer, are the two scalars adopted by the partially premixed model. The position of the flame front is determined by the premixed reaction-progress variable. The mixture is burned behind the flame front ($C = 1$) using the equilibrium or laminar flamelet mixture fraction solution. In the flame front, ($C = 0$), the temperature, species mass fractions and the density are calculated from the unburnt mixture fraction. Within the flame ($0 < C < 1$), a linear combination of the unburnt and the burnt mixtures is utilized. The reaction progress variable has a transport equation of the form

C. Aigbavboa et al. (Eds.): Sustainable Education and Development, pp. 818-832, 2024.
https://doi.org/10.1007/978-3-030-68836-3 1

$$\frac{\partial}{\partial t}(\rho C) + \frac{\partial}{\partial x_k}(\rho u_k C) = \frac{\partial}{\partial x_k}\left[\rho D \frac{\partial C}{\partial x_k}\right] + \rho \dot{w}_c \quad (6)$$

where the progress variable that models the "progress "of the reaction is denoted by C. $\dot{w}_c$ and D represent the chemical source term and the molecular scalar diffusivity, respectively. The CRECK reaction mechanism of Ranzi et al. (2012) which contained 113 species and 1909 reactions was used to simulate the kinetics of the chemical reactions. The mechanism is well-built and can manage the high temperature pyrolysis, the partial oxidation, and the combustion of hydrocarbon fuels including up to three carbon atoms. Alkanes, alkynes, and alcohols are examples of hydrocarbon and oxygenated fuels that the process has been successfully applied to in various instances, according to Ranzi et al.

Radiationand Soot models

The radiative transfer equation (RTE), which appears as a sink in the enthalpy equation (equation 3), must be solved in order to ascertain the fraction of heat lost in flames as a result of radiation. The transit of incoming and outgoing radiation intensity through the computational domain is described by the governing equation for radiative heat transfer, which is represented as (Modest, 2003)

$$\frac{dI(\vec{r},\vec{s})}{ds} + (a+\sigma_s)I(\vec{r},\vec{s}) = an^2\frac{\sigma T^4}{\pi} + \frac{\sigma_s}{4\pi}\int_0^{4\pi} I(\vec{r},\vec{s}')\,\Phi(\vec{s},\vec{s}')d\Omega' \quad (7)$$

where$\vec{s}$ and $\vec{s}'$and $\vec{r}$are the direction vector, the scattering direction vector and the position, respectively. $\sigma_s$is the scattering coefficient, s is the path length,a is the absorption, n is the refractive index, T is the local temperature,I is the radiation intensity, Ω' is the solid angle, Φ is the phase function and σ is the Stefan-Boltzmann constant which is given as 5.672×10^{-8} W/m^2-K^4. The Moss-Brookes-Hall model (Hall et al., 1999) implemented in the Fluent code was used to model the soot in the flames where the soot nucleation and growth are modelled on acetylene (C_2H_2) as the soot precursor and the gas phase specie. Soot formation and oxidation compete in a flame and the quantity of soot that is emitted will be dependent upon the balance between these two processes. They can be expressed mathematically as

$$\frac{dM}{Dt} = \left(\frac{dM}{dt}\right)_{Inc.} + \left(\frac{dM}{dt}\right)_{Gro.} + \left(\frac{dM}{dt}\right)_{Oxi.} \quad (8)$$

where M denotes the soot mass density, the first and the second terms on the right denote the rates of soot formation (i.e., inception and growth) and the third term denotes the rate of soot oxidation.

C. Aigbavboa et al. (Eds.): Sustainable Education and Development, pp. 818-832, 2024.
https://doi.org/10.1007/978-3-030-68836-3 1

2.2 Computational Methods

The experimental work by Huang & Yang (1996), which examined the structure of a wake-stabilized cross flow propane flame in various regimes as well as the species concentration and the thermal field of the flames, served as the basis for the computer simulation used in this study. The simulation was carried out on a three-dimensional structured hex mesh created with the use of the meshing tool ANSYS-Icem, which in general yields more accurate results with fewer computational cells. Figure 2 shows the size of the computational domain which was based on the wind tunnel test section (30 x 30 x 110 cm^3) such that the origin was placed at center of the burner outlet. This was done in order to reduce the impact of the lower and upper boundaries of the computational domain. The burner was modeled as a cylindrical tube with measurements that matched those of the experimental set-up. In order to limit the impact of the flare-pipe on the flow at the inlet boundary and to allow for the assumption of a fully developed flow in the downstream boundary, the tube was placed about 240 mm from the cross-flow inlet border and extended 180 mm into the combustion zone. In order to guarantee that the solution is independent of the mesh size, a mesh independent study was conducted and a mesh density of 2.52 million cells was found to be optimal. Boundary conditions were chosen as follows: On the *z—y* plane, which corresponded to the cross-flow inlet, a uniform velocity profile and 0.18% turbulence intensity was specified. On the *z—x* plane, a no-slip wall boundary condition was specified at the back and the front of the box. Further downstream, outflow conditions were specified such that a zero value for the normal gradient for all flow variables, except pressure, were implemented. A uniform fuel velocity was implemented at the pipe inletwith a 10% turbulence intensity, which is representative of fully developed pipe flow. At the pipe walls no-slip wall boundary conditions were specified. On the *z—x* planes, no-slip wall and stationary boundary conditions were also implemented which represented the box enclosure. Similar conditions were also specified at the bottom and top of the box corresponding to the *x—y* planes. A total of 18flamelets over a scalar dissipation rate 0.0002 -20 s^{-1} in scalar dissipation steps of 2.2 s^{-1} was used, which has been demonstrated to give an acceptable level of accuracy for the situation under consideration (Lawal et al., 2013). The LES calculations was carried out in time step sizes of 1.2 x 10E-5, for a flow time of 1.50 s in order to achieve a pseudo-steady state solution. This is about 2 flow residence times across the solution domain and all residuals were observed to be lower than 10^{-6}. The model by Smagorinsky (Smagorinsky, 1963) was used to approximate the sub grid scale turbulence in the flow domain and the kinetics of propane reactions was based on the CRECK reaction mechanism of Ranzi et al. (Ranzi et al., 2012).

3 RESULTS AND DISCUSSIONS

3.1. Flame structure

Wake-stabilized flames can be observed to be only loosely attached to the lee-side of the fuel pipe, suggesting that they are occasionally lifted and reattached. Given this finding, Huang and Yang (1996) used the partially premixed model to simulate the wake stabilized flame. The two models, the LES and

C. Aigbavboa et al. (Eds.): Sustainable Education and Development, pp. 818-832, 2024.
https://doi.org/10.1007/978-3-030-68836-3 1

the RANS models, have been compared to the experimental data, and the predictions of the flame structure have been compared to the observations made by Huang and Yang. Figure 3 (a) and Figure 3 (b) shows a comparison of the titanium-tetrachloride flow visualization of the flame as observed by Huang and Yang (1996) with the predicted flame contours obtained from the LES and the RANS simulation and it is clear from this outcome that the LES model was far more successful than the RANS model at simulating the wake-stabilized flame's physical structure. It is interesting to see that the LES model does a good job of simulating the curve created by the flame at the wake of the pipe as it periodically separates from and reattaches to the wake of the burner. This behavior resembles that of a straight jet flame's lift-off and reattachment phases, which are principally caused by the action of fuel and air premixing at the flame's base.

3.2. Flame temperature and species

Figure 4 (a) and Figure 4 (b) shows the flame temperature predictions using the RSM and LES turbulence models together with the partially premixed combustion model at two locations in the flame, and the predictions have been validated using Huang and Yang's experimental findings. It can be seen that the LES predictions are better than that of the RSM at the upstream locations of x = 8.2 mm, z = 0, and x = 8.2 mm, z = 7 mm. This can be clearly seen for the temperature prediction at x = 8.2 mm, z = 7 mm where it can be seen that the large spreading rate produced by the RSM between -6 mm < y < 0, was successfully handled by LES. The peak temperature predicted by the LES, however, was within the same range as that predicted by the RSM. Similarly, Figure 5 (a) and Figure 5 (b) shows the predictions of the pollutant species from the flame using the RSM and LES turbulence models together with the partially premixed combustion model at the same locations in the flame. The predictions for CO have been validated against the work of Huang and Wang, the NO predictions, on the other hand, were not validated because Huang and Yang did not disclose experimental data on NO. The predictions, however, remain within the ranges noted in the literature (Bandaru and Turns, 2000, Paul et al., 2021). As we can see from the figures, the predictions of the CO

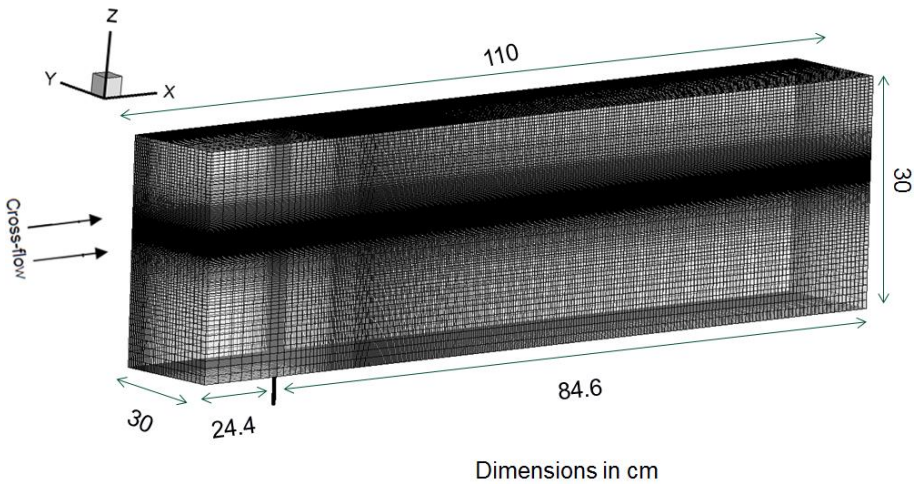

Figure 2.Mesh of the wind tunnel test section for the Huang and Yang experiment simulation

C. Aigbavboa et al. (Eds.): Sustainable Education and Development, pp. 818-832, 2024.
https://doi.org/10.1007/978-3-030-68836-3 1

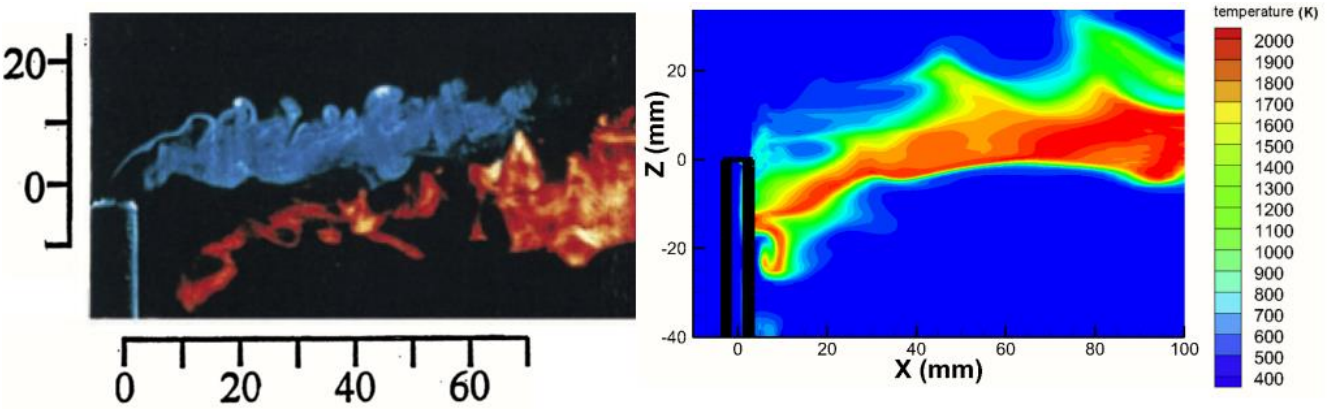

(*a*)

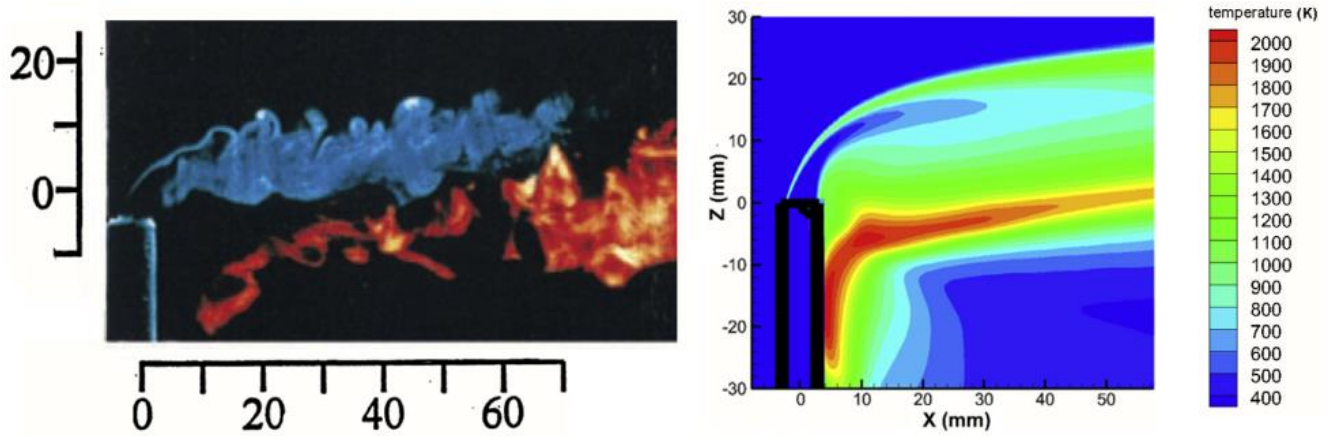

(*b*)

Figure 3.Comparison of experimental flame with (a) LES prediction (b) RANS prediction for u_j=5.78 m/s and u_{cf}=4.86 m/s

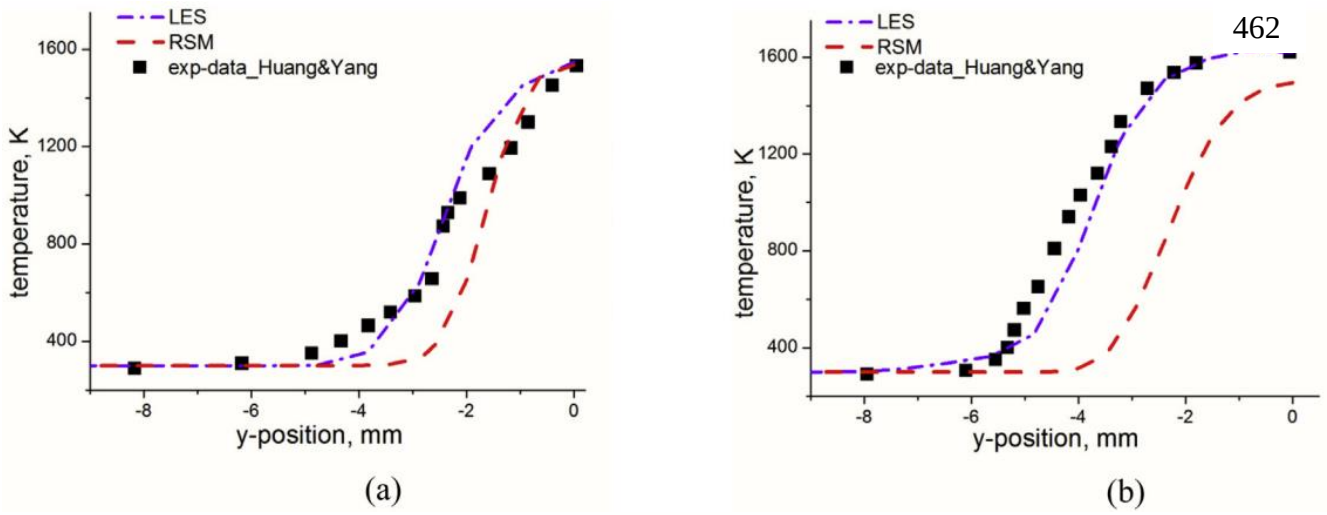

Figure 4. Predictions of the flame temperature at (a) x = 8.2mm, z = 0 (b) x = 8.2mm, z = 7mm

C. Aigbavboa et al. (Eds.): Sustainable Education and Development, pp. 818-832, 2024.
https://doi.org/10.1007/978-3-030-68836-3 1

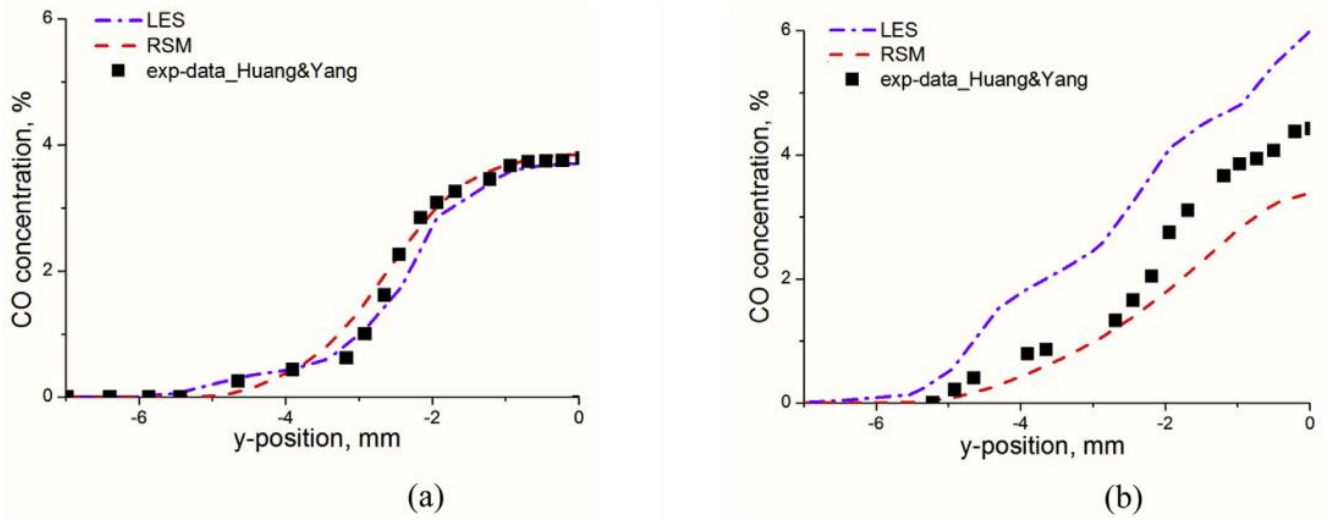

Figure 5. Predictions of the flame CO concentration at (a) x = 8.2mm, z = 0 (b) x = 8.2mm, z = 7mm

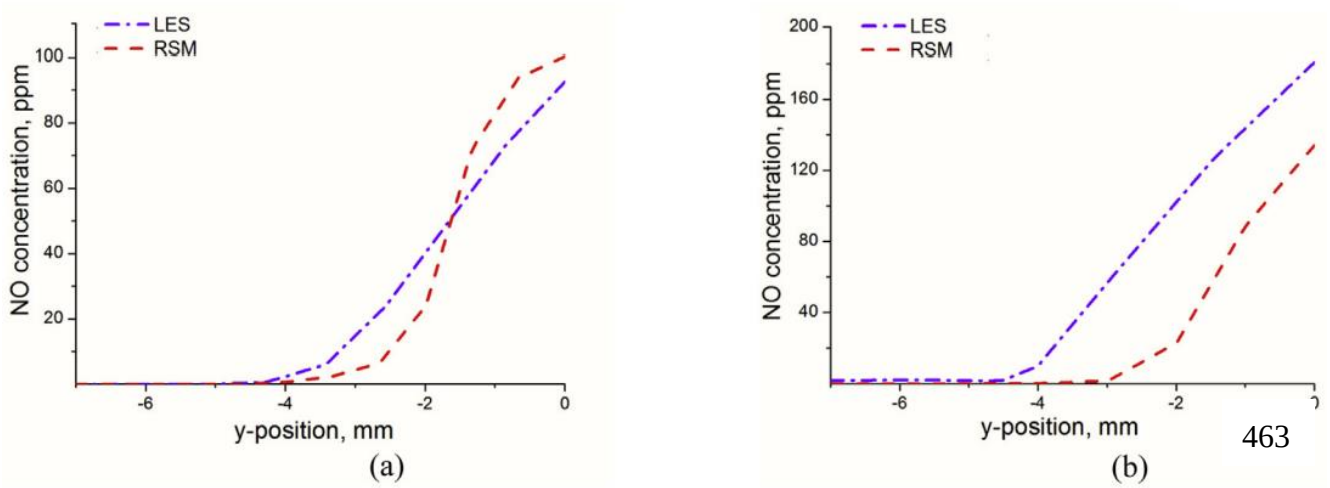

Figure 6. Predictions of the flame NO concentration at (a) x = 8.2mm, z = 0 (b) x = 8.2mm, z = 7mm

concentrations made by the RSM and the LES were both very good at at x = 8.2, z = 0, with both models producing an almost perfect fit to the experimental data at this location. This is pleasantly unexpected considering how challenging it is to predict carbon monoxide in flames because it typically develops very slowly in flames and achieves partial equilibrium much later. The use of a tiny mesh, a narrow range of scalar dissipation rates and a small scalar dissipation step (0.0002 - 22 s^{-1} in scalar dissipation steps of 2.4 s^{-1}) may all have contributed to the improved predictions of carbon monoxide concentrations. Lawal et al. (2013) have shown that this range of scalar dissipation steps is enough for accounting for the relaxation effects on the pollutant species.

C. Aigbavboa et al. (Eds.): Sustainable Education and Development, pp. 818-832, 2024.
https://doi.org/10.1007/978-3-030-68836-3 1

4 CONCLUSION

The experimental work of Huang and Yang has been numerically simulated in three dimensions in this work, leading to the following findings:

- While both models accurately predicted the peak temperatures at the measurement locations investigated, the LES model outperformed the RSM in terms of predicting the temperature trend. With the exception of carbon monoxide at the tested location close to the nozzle, the LES performed better at predicting species. In general, the RSM provides a fair prediction of the thermo-chemical characteristics of the flame, making it an appealing substitute for the significantly more expensive LES.

- The appearance and the thermochemical characteristics of wake stabilized cross flow propane flames can be accurately predicted by the partially premixed combustion model.

- The Moss-Brookes-Hall soot model and the CRECK reaction mechanism can work well in conjunction with the partially premixed model for predicting cross flow propane flames.

This work has been able to contribute to the pool of available knowledge on flares by providing the flame structure and the thermochemical properties of propane combustion in a cross flow since prev 464
works that have been done on gas flares have focused mainly on methane. However, once there is enough experimental data on cross-flow wake-stabilized flames, more research will need to be done to examine how the soot and radiation models affect the performance of the two turbulence models explored in this paper.

5 ACKNOWLEDGEMENT

A. Aboje wishes to acknowledge the contributions made by Alexander Pranzitelli, Sandy Black and Porter Richard.

C. Aigbavboa et al. (Eds.): Sustainable Education and Development, pp. 818-832, 2024.
https://doi.org/10.1007/978-3-030-68836-3 1

6 REFERENCES

ANSYS-Fluent R2. (2020). *Theory Guide*. Version 14.5 Sheffield, U.K., ANSYS-Fluent Europe, Limited.

Bandaru, R. V., & Turns, S. R. (2000). Turbulent jet flames in a crossflow: effects of some jet, crossflow, and pilot-flame parameters on emissions. *Combustion and Flame*, *121*, 137–151.

Botros, P. E., & Brzustowski, T. A. (1979). An experimental and theoretical study of a turbulent diffusion flame in cross-flow. *Proceedings of the Combustion Institute*, *17*, 389–398.

Castineira, D., & Edgar, T. F. (2008). Computational fluid dynamics for simulation of wind-tunnel experiments on flare combustion systems. *Energy and Fuels*, *22*, 1698–1706.

Eric, D. L., Colin, J. F., & Robert, B. J. (2022). Methane and NOx Emissions from Natural Gas Stoves, Cooktops, and Ovens in Residential Homes. *American Chemical Society (ACS)*, *56*(4), 2529–2539.

Escudier, M. P. (1971). Aerodynamics of a burning turbulent gas jet in a crossflow. *Combustion Science and Technology*, *4*, 293–301.

Ferziger, J. H. (1976). Large eddy simulations of turbulent flows. *American Institute of Aeronautics and Astronautics*, *14*, 75–76.

Fiveland, W. A. (1984). Discrete-ordinates solution of the radiative heat transport-equation for rectangular enclosures. *ASME Journal of Heat Transfer*, *106*, 699–706.

Gollahalli, S. R., & Nanjundappa, B. (1995). Burner wake stabilized gas jet flames in cross-flow. *Combustion Science and Technology*, *109*, 327–346.

Hall, R. J., Smooke, M. D., & Colket, M. B. (1999). *In Physical and chemical aspects of combustion*. Gordon and Breach.

Huang, R. F., & Yang, M. J. (1996). Thermal and concentration fields of burner-attached jet flames in cross flow. *Combustion and Flame*, *105*, 211–244.

Ilya, G., Vyacheslav, Z., & Konstantin, A. (2022). Experimental Study of Methane Combustion Efficiency in a High-Enthalpy Oxygen-Containing Flow. *Applied Sciences*, *12*(2), 899.

John, A. F. (2023). *Global Gas Flaring Reduction Partnership (GGRP): Zero routine flaring by 2030 initiative*. https://www.worldbank.org/en/programs/gasflaringreduction

C. Aigbavboa et al. (Eds.): Sustainable Education and Development, pp. 818-832, 2024.
https://doi.org/10.1007/978-3-030-68836-3 1

Launder, B. E., Reece, G. J., & Rodi, W. (1975). Progress in the development of a Reynolds-stress turbulence closure. *Journal of Fluid Mechanics, 68,* 537–566.

Lawal, M. S., Fairweather, D. B., Ingham, D. B., Ma, L., Pourkashanian, M., & Williams, A. (2010). Numerical study of emission characteristics of a jet flame in cross-flow. *Combustion Science and Technology, 182,* 1491–1510.

Lawal, M. S., Fairweather, D. B., Ingham, D. B., Ma, L., Pourkashanian, M., Williams, A., & Gogolek, P. (2013). CFD predictions of wake-stabilised jet flames in a cross-flow. *Energy, 53,* 259–269.

Modest, M. F. (2003). *Radiative Heat Transfer*. London, Academic Press.

Paul, L., Moussa, K., & Fadiala, D. (2021). Methane gas emissions from savanna fires. *Biogeosciences, 18*(23), 6229–6244.

Pierce, C., & Moin, P. (2004). Progress-Variable approach for Large-Eddy Simulation of non-premixed turbulent combustion. *Journal of Fluid Mechanics, 70,* 502–504.

Ranzi, E., Frassoldati, A., & Grana, R. (2012). Hierarchical and comparative kinetic modelling of laminar flame speeds of hydrocarbon and oxygenated fuels. *Progress in Energy and Combustion Science, 38,* 468–501.

Smagorinsky, J. (1963). General circulation experiments with the primitive equations I: the basic equations. *Weather Review, 91,* 99–164.

Sullivan, J. (2023). *The Intergovernmental Panel on Climate Change (IPCC): 30 Years of informing global climate action*. https://unfoundation.org/blog/post/intergovernmental-panel-climate-change-30-years-informing-global-climate-action/

C. Aigbavboa et al. (Eds.): Sustainable Education and Development, pp. 818-832, 2024.
https://doi.org/10.1007/978-3-030-68836-3 1